Energy Efficient Base Station Density Analysis for Heterogeneous Networks with eICIC

Yanzan Sun, Wenqing Xia, Yating Wu, Tao Wang, and Yong Fang
Shanghai Institute for Advanced Communication and Data Science, Shanghai Key Laboratory of Specialty Fiber Optics and Optical Access Networks, Shanghai University, Shanghai 200072, China
Email: {yanzansun, ytwu, twang, yfang}@shu.edu.cn; wenqingxia_1993@163.com

Abstract —Heterogeneous Networks (HetNets), where low-power nodes are overlaid on the traditional macro base station (MBS), have been investigated as a promising paradigm to support the deluge of data traffic with higher spectral efficiency and energy efficiency. However, the density of BS and the inter-tier interference are the two important influence factors for the network performance implementation. As for the inter-tier interferences, time domain Enhanced Inter-cell Interference Coordination (eICIC) technique is adopted to mitigate it and improve the system capacity for HetNets in LTE-Advanced. In this, the reasonable configuration of the density of base stations is very essential for the network performance improvement, especially for the network energy optimization. Thus in this paper, we deduce the closed-form of network energy efficiency as a function of the density of BSs with eICIC technology based on stochastic geometry theory. Then the impacts of the BSs density on the network energy efficiency is further analyzed by simulation. Simulation results show that the theoretical derivation is verified well by Monte Carlo simulation and the reasonable BSs density configuration can improve the network energy efficiency effectively.

Index Terms—HetNets, eICIC, energy efficiency, stochastic geometry

I. INTRODUCTION

Data traffic demand in cellular networks has kept on increasing at an exponential rate nowadays, and it will continue to be strong at least in this decade [1]. However, with the scarce spectrum resources, the large demand of data traffic is impossible to be satisfied by adding the spectrum bandwidth. To solve this problem, heterogeneous networks (HetNets) deployment is a trend. Heterogeneous network is a new network structure that small base stations (SBSs) such as pico, femto and relay are overlaid on the traditional macro base stations (MBSs) and share the same spectrum with MBSs. In this way, the reuse per unit area of the existing spectrum is increased cost-effectively and the deluge of data traffic can be supported with higher spectral efficiency [2].

Manuscript received August 30, 2017; revised February 1, 2018.
This work was supported by the National Natural Science Foundation of P.R. China under Grant No 61501289, 61671011, 61401266, 61673253, 61420106011; the Research Fund for the Doctoral Program of Higher Education of China under Grant No 20133108120015 and the Shanghai Science and Technology Development Funds under Grant No 17010500400 respectively.
Corresponding author email: yanzansun@shu.edu.cn
doi:10.12720/jcm.13.2.60-66

In heterogeneous networks consisted by MBS and Pico Base Stations (PBSs), PBSs usually adopt Cell Range Expansion (CRE) to balance the load between MBSs and PBSs. CRE is a technique that adds a bias value to Reference Signal Received Power (RSRP) from PBSs so that more users will choose the PBSs to associate [3], [4]. Nevertheless, the pico CRE users which are located in the expanded area of the PBSs will suffer severe inter-tier downlink interference from MBSs. To cope with the inter-tier interference issues, Enhanced Inter-cell Interference Coordination is an important feature in LTE-Advanced, which relies on Almost Blank Subframe (ABS) to mitigate the inter-tier downlink interference between macrocell and picocell. In eICIC standards, each MBS remains silent for ABSs, over which PBS can schedule CRE area users with reduced interference [5], [6].

In addition, with the drastic growth of network capacity demand, dense deployment of Base Stations (BSs) (especially SBSs) in HetNets offers a cost-effective way to increase the reuse per unit area of the existing spectrum, which significantly improves the network capacity [7]. However, deploying too many BSs will cause a lot of energy consumption and a mess of interference unavoidably. Therefore, it is very necessary to configure reasonable BS density in HetNets from the point of view of network energy efficiency optimization.

The SBS density optimization for network capacity improvement was studied respectively in [8]-[11]. Specifically, in [8], the closed form solution of the network capacity as a function of micro BS density is derived on the basis of stochastic geometry model and the optimal micro BS density was obtained to maximize the network capacity. In [9], a general and tractable framework for modeling and analyzing joint resource partitioning and offloading in a two-tier HetNets based on stochastic geometry was investigated, where the ABS ratio and CRE bias were optimized together to maximize the network rate coverage. The authors of [10] verified that HetNets with low-power nodes (i.e., small cells, which may be employed indoors or outdoors) was a simpler cost-effective way for system capacity expansion compared to conventional cell splitting. In [11], the impact of the SBS density on Spectral Efficiency (SE) and Area Spectral Efficiency (ASE) was studied respectively, and the SBS density was optimized to maximize the SE and ASE jointly.

The BS density optimization for network energy efficiency enhancement was investigated respectively in [2], [12]-[15]. To be specific, the BS density for maximizing network energy efficiency was optimized by stochastic geometry theory for homogeneous network with different network loads in [12]. In [13], a density threshold of small cells in ultra-dense cellular networks was investigated considering the backhaul network capacity and energy efficiency. The authors of [14] came up with an approximation algorithm to solve the intractable user association problem by controlling the SBS density dynamically. Furthermore, [2] had proved that not only the density of SBS had a notable impact on the network energy efficiency, the density of MBS can also affect the network energy efficiency. The authors of [15] optimized the SBS density and MBS density together through traffic-aware sleeping strategies to enhance the network energy efficiency. However, these works did not consider the eICIC for the inter-tier interference coordination in HetNets.

Since the randomness of the BSs deployment in reality, the traditional hexagonal cellular model cannot reflect the real network deployment precisely [16]. For this, the authors of [17] proposed a tractable analytical model for the cellular network deployment that the location distribution of BSs was modeled as spatial Poisson Point Process (PPP). Based on the PPP model, the network performance such as average achievable data rate, coverage probability, rate coverage and energy efficiency can be derived as closed-form expressions.

The main contributions of this paper are as follows. Firstly we deduce the closed-form expression of the network energy efficiency based on the stochastic geometry theory. Then the impacts of SBS density and MBS density on the network energy efficiency are analyzed in detail.

The rest of this paper is organized as follows. The system model is described in Section II. The analytical model is given in Section III, where we can obtain the closed-form expression of network energy efficiency. Numerical results and discussions are presented in Section IV. Concluding remarks are given in Section V.

II. System Model

A two-tier HetNets consisting of MBSs with higher transmission power and PBSs with lower transmission power is considered, as shown in Fig. 1. Let $k \in \{1,2\}$ to denote the tier index. Without any loss of generality, let the macrocells be tier 1 and the picocells constitute tier 2. We assume that the MBSs and PBSs are spatially located according to a homogeneous Poisson point process (PPP) Φ_m and Φ_p with density λ_m and λ_p respectively in the Euclidean plane. The UEs are also distributed according to a different independent PPP Φ_u with density λ_u. To mitigate the downlink interference from MBS to pico CRE users, ABS scheme is adopted in MBS, where all the subframes are configured as the ABS subframes and the non-ABS subframes in time domain respectively. We denote θ to be the ABS ratio, i.e. the proportion between the amount of ABS subframes and the number of the entire subframes. The transmission power of MBS in ABS and Non-ABS subframes are $0w$ and P_m respectively. In ABS subframe, picocells still suffer from Cell-specific Reference Symbol (CRS) interference which is transmitted at regular intervals by MBS. Therefore, we assume that CRS interference cancellation is ignored in pico for analysis simplicity. The transmission power of PBSs is denoted as P_p.

We consider a cell association based on the maximum biased Reference Signal Received Power (RSRP), where a User Equipment (UE) is associated with the strongest BS in terms of the biased received RSRP at the user. In this paper, the association bias for MBS is assumed to be unity ($B_m = 0\text{dB}$) and that for PBS is pico Cell Range Expansion (CRE) bias depicted as B_p , where $B_p \geq 0\text{dB}$. According to the cell association, all the UEs are divided into three different types as shown in Fig. 1: the type of MBS UEs contains the users connected to the macrocell, the type of PBS CRE UEs corresponds to the users located in the expanded region of the picocell (i.e. the users receiving a higher RSRP from the MBS than from the PBS) and the type of PBS center UEs comprises the users distributed in the original coverage of picocell (i.e. the users receiving a higher RSRP from the PBS than from MBS). Each MBS remains silent on ABS subframes, over which PBS can schedule PBS CRE UEs with reduced interference. The Non-ABS subframes will be assigned to the MBS UEs and the corresponding subframes for pico are allocated to the PBS center UEs.

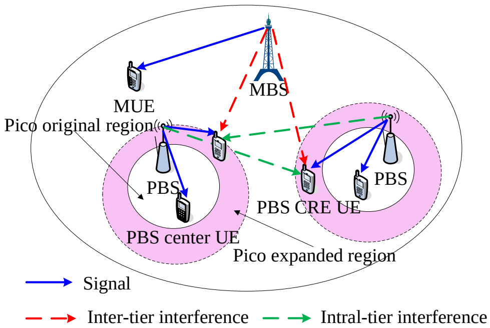

Fig. 1. The network scenario

Without loss of generality, we conduct analysis on a typical UE at the origin. This is allowed by Slivyak's theorem, which states that there is no difference in property observed either at a point of the PPP or at an arbitrary point [9]. We adopt the index $l \in \mathbf{L} = \{m_u, p_c, p_e\}$ to denote the indication of the above three types of UEs respectively, where m_u

represents MBS UEs, p_c denotes the PBS center UEs and p_e signifies PBS CRE UEs.

The received signal power of a typical UE l from a BS of k th tier at a distance of r_l can be represented as $P_k h r_l^{-\alpha}$, where P_k is the transmission power of BS in the k th tier, the variable h denotes the channel fast fading gain, which is modeled as Rayleigh distributed with average unit power, i.e. $h \sim \exp(1)$, the term α is the large scale path loss exponent, which is assumed to be the same in both of the two tiers for analysis simplicity. Thus, the SINR of a typical UE l according to its user type can be expressed as:

$$\gamma_l = \begin{cases} \dfrac{P_m h r_l^{-\alpha}}{\sum_{k=1}^{2} I_{k,l} + \sigma^2}, & \text{if } l = m_u \\ \dfrac{P_p h r_l^{-\alpha}}{\sum_{k=1}^{2} I_{k,l} + \sigma^2}, & \text{if } l = p_c \\ \dfrac{P_p h r_l^{-\alpha}}{I_{2,l} + \sigma^2}, & \text{if } l = p_e \end{cases} \tag{1}$$

where $I_{k,l}$ denotes the interference from the k th tier to UE l .

We restrict that the PBS CRE UEs can only be scheduled by PBS in the subframes that are corresponding to the MBS ABS subframes. Therefore, when $l{=}p_e$, the interference from MBSs, i.e. tire 1, can be omitted when the CRS interference cancellation is utilized in pico. That is why we just consider $I_{2,l}$, i.e. the intral-tier interference from pico tier, in the denominator of the SINR expression when $l{=}p_e$.

III. Analytical Model

A. User Association Probability

We assume that the nearest distances from a typical UE to a PBS and a MBS are denoted by r_p and r_m respectively. Thus, the user type of this typical UE can be defined according to the relationship between the received signal strength from its nearest MBS and PBS respectively as (2) below:

$$l = \begin{cases} m_u, \text{when } P_m h r_m^{-\alpha} > B_p P_p h r_p^{-\alpha} \\ p_c, \text{when } P_p h r_p^{-\alpha} > P_m h r_m^{-\alpha} \\ p_e, \text{when } P_p h r_p^{-\alpha} < P_m h r_m^{-\alpha} < B_p P_p h r_p^{-\alpha} \end{cases} \tag{2}$$

According to the Lemma 1 in [9], corresponding to the user type, the user association probability can be defined as $A_l = \Pr ob[l \in L]$, which is given as below:

$$A_l = \begin{cases} \dfrac{\rho_1}{\rho_1 + \left(B_p \hat{P}_p\right)^{2/\alpha} \rho_2}, \text{when } l = m_u \\ \dfrac{\rho_2}{\rho_2 + \left(\hat{P}_m\right)^{2/\alpha} \rho_1}, \text{when } l = p_c \\ \dfrac{\rho_2}{\rho_2 + \left(B_p^{-1}\hat{P}_m\right)^{2/\alpha} \rho_1} - \dfrac{\rho_2}{\rho_2 + \left(\hat{P}_m\right)^{2/\alpha} \rho_1}, \text{when } l = p_e \end{cases} \tag{3}$$

where $\hat{P}_p = P_p / P_m$, $\hat{P}_m = P_m / P_p$, $\rho_1 = \lambda_m / \lambda_u$ is the ratio between the MBS density and user density in the Euclidean plane, and $\rho_2 = \lambda_p / \lambda_u$ is the ratio of the PBS density to user density in the Euclidean plane.

B. Distribution of Serving BS Distance

According to the Lemma 2 in [9], corresponding to the user type, the distribution of the distance r_l between a typical UE l and its serving BS can be expressed as (4) respectively:

$$\begin{aligned} f_{m_u}(r_l) &= \frac{2\pi r_l \lambda_m}{A_{m_u}} \exp\left[-\pi r_l^2 \left(\lambda_m + \left(B_p \hat{P}_p\right)^{2/\alpha} \lambda_p\right)\right] \\ f_{p_c}(r_l) &= \frac{2\pi r_l \lambda_p}{A_{p_c}} \exp\left[-\pi r_l^2 \left(\lambda_p + \left(\hat{P}_m\right)^{2/\alpha} \lambda_m\right)\right] \\ f_{p_e}(r_l) &= \frac{2\pi r_l \lambda_p}{A_{p_e}} \left\{\exp\left[-\pi r_l^2 \left(\lambda_p + \left(B_p^{-1} \hat{P}_m\right)^{2/\alpha} \lambda_m\right)\right] \right. \\ &\quad \left. - \exp\left[-\pi r_l^2 \left(\lambda_p + \left(\hat{P}_m\right)^{2/\alpha} \lambda_m\right)\right]\right\} \end{aligned} \tag{4}$$

C. The Ratio of Almost Blank Subframe

We set the value of the ABS ratio θ to be the proportion between the PBS CRE UE association probability and all the PBS user association probability (i.e. the sum of the PBS CRE UE association probability and the PBS center UE association probability) as shown in formula (5).

$$\theta = \frac{A_{p_c}}{A_{p_c} + A_{p_e}} \tag{5}$$

D. Average Achievabe Downlink Rate

Assume that the network system adopts full buffer traffic model and all the users in the coverage of a BS share the entire frequency resource equally. Thus, the mean achievable downlink data rate of a typical UE l can be represented as follows:

$$R_l = \frac{W_l}{E[N_l]} E\left[\log_2(1 + \gamma_l)\right] \tag{6}$$

where N_l is the mean load in a Voronoi cell and the expectation of N_l is $E[N_l] = (A_l / \rho_k) + 1$, when $l{=}m_u$, then $\rho_k = \rho_1$ and when $l \in \{p_c, \rho_e\}$, then

$\rho_k = \rho_2$. W_l is the time-frequency resource that is allocated to user l and its value depends on the user type of user l . Specifically, when l=p_e , then $W_l = \theta W$ and when $l \in \{m_u, p_c\}$, then $W_l = (1\text{-}\theta)W$.

Based on the analysis above, we get Lemma 1 in the following:

Lemma 1: The average achievable downlink rate of a typical UE l can be further deduced as:

$$R_l = \frac{2\pi\lambda_l W_l}{A_l N_l}\int_0^\infty\int_0^\infty \exp\left(-\varphi_l - \pi r_l^2 C_l\right) f_l\left(r_l\right)dr_l dt \quad (7)$$

where $\tau = 2^t - 1, \quad \varphi_l = -\tau\sigma^2 r_l^2 P_k^{-1}$.

$$C_l = \begin{cases} \lambda_m Z(\tau,\alpha,1) + \lambda_p Z(\tau,\alpha,B_p), \text{when } l\text{=}m_u \\ \lambda_m \hat{P}_m Z(\tau,\alpha,1) + \lambda_p Z(\tau,\alpha,1), \text{when } l\text{=}p_c \\ \lambda_p Z(\tau,\alpha,1), \text{when } l\text{=}p_e \end{cases},$$

where $Z(\tau,\alpha,\beta) = \tau^{2/\alpha}\int_{(\beta/\tau)^{2/\alpha}}^\infty \frac{1}{1+x^{\alpha/2}}dx$.

Corollary 1: With noise ignored, and set the large scale path loss exponent α=4 , the average achievable downlink rate of a typical UE l can be simplified respectively according to its user type as follows:

$$\begin{aligned} R_{m_u} &= \frac{(1-\theta)W}{A_{m_u}N_{m_u}}\int_0^\infty \frac{1}{Q(\tau,4,1)+\frac{\rho_2}{\rho_1}Q\left(\hat{P}_p\tau,4,B_p\hat{P}_p\right)}dt \\ R_{p_c} &= \frac{(1-\theta)W}{A_{p_c}N_{p_c}}\int_0^\infty \frac{1}{Q\left(\hat{P}_m\tau,4,\hat{P}_m\right)+\frac{\rho_1}{\rho_2}Q(\tau,4,1)}dt \\ R_{p_e} &= \frac{\theta W}{A_{p_e}N_{p_e}}\int_0^\infty \frac{1}{Q(\tau,4,1)+\left(B_p^{-1}\hat{P}_m\right)\frac{\rho_1}{\rho_2}} \\ &\quad -\frac{1}{Q(\tau,4,1)+\hat{P}_m\frac{\rho_1}{\rho_2}}dt \end{aligned} \quad (8)$$

where $Q(\tau,4,x) = \sqrt{x} + \sqrt{\tau}\tan^{-1}\left(\sqrt{\tau/x}\right)$.

E. BS Power Cconsumption and Energy Efficiency

Generally, BS consists of two types of power consumptions: static power consumption and transmit power consumption [2]. Then for the k th tier, a BS power consumption can be given as follows:

$$P_k = P_{k,s} + \xi_k P_{k,t} \quad (9)$$

where $P_{k,s}$ is the static power consumption of a BS in the k th tier, which is caused by signal processing, battery backup, as well as site cooling, and is independent with the BS transmit power. $P_{k,t}$ is the transmit power of a BS for data transmission in the k th tier, and ξ_k is the load-dependent power consumption coefficient of a BS in the k th tier.

Note that the transmit powers of MBS in ABS subframe and Non-ABS subframe are different. Therefore, the system power consumption in ABS subframe and Non-ABS subframe will not be the same. Thus, we decompose the system power consumption into two parts: the system power consumption in ABS subframe P_{abs} and the system power consumption in Non-ABS subframe P_{non_abs} . Especially, the transmit power consumption of MBS for data transmission in ABS subframe is assumed to be zero due to its silence in ABS subframe. Combined with (9) and the density of MBS and PBS, P_{abs} and P_{non_abs} can be obtained in the following respectively:

$$\begin{aligned} P_{abs} &= \lambda_m P_{1,s} + \lambda_p P_{2,s} + A_{p_e}\lambda_u P_{2,t} \\ &= \lambda_m P_{m,s} + \lambda_p P_{p,s} + A_{p_e}\lambda_u P_{p,t} \end{aligned} \quad (10)$$

$$\begin{aligned} P_{non\_abs} &= \lambda_m P_{1,s} + A_{m_u}\lambda_u P_{1,t} + \lambda_p P_{2,s} + A_{p_c}\lambda_u P_{2,t} \\ &= \lambda_m P_{m,s} + A_{m_u}\lambda_u P_{m,t} + \lambda_p P_{p,s} + A_{p_c}\lambda_u P_{p,t} \end{aligned} \quad (11)$$

Considering the ABS ratio θ, the system total power consumption can be derived as:

$$P_{total} = \theta P_{abs} + (1-\theta)P_{non\_abs} \quad (12)$$

F. Network Energy Efficiency

The network energy efficiency can be defined as the ratio of the effective system capacity over the system total power consumption:

$$\eta_{EE} = \frac{R_{total}}{P_{total}} = \frac{R_{total}}{\theta P_{abs} + (1-\theta)P_{non\_abs}} \quad (13)$$

For convenient derivation, we set α=4 , σ^2=0 . Then, combining (8), (9)-(13), the expression of the network energy efficiency is obtained as follows:

$$\begin{aligned} \eta_{EE} &= \frac{R_{total}}{P_{total}} = \frac{\left(R_{m_u}A_{m_u} + R_{p_c}A_{p_c} + R_{p_e}A_{p_e}\right)\lambda_u}{P_{total}} \\ &= \frac{\lambda_u}{P_{total}}\int_0^\infty \frac{(1-\theta)W/N_{m_u}}{Q(\tau,4,1)+\frac{\rho_2}{\rho_1}Q\left(\hat{P}_p\tau,4,B_p\hat{P}_p\right)} \\ &\quad + \frac{(1-\theta)W/N_{p_c}}{Q\left(\hat{P}_m\tau,4,\hat{P}_m\right)+\frac{\rho_1}{\rho_2}Q(\tau,4,1)} - \frac{\theta W/N_{p_e}}{Q(\tau,4,1)+\hat{P}_m\frac{\rho_1}{\rho_2}} \\ &\quad + \frac{\theta W/N_{p_e}}{Q(\tau,4,1)+\left(B_p^{-1}\hat{P}_m\right)\frac{\rho_1}{\rho_2}}dt \end{aligned} \quad (14)$$

where

$$\lambda_u / P_{total} = 1 \Big/ \left\{ \rho_1 P_{m,s} + \rho_2 P_{p,s} + \theta A_{p_e} P_{p,t} + (1-\theta)\left(A_m P_{m,t} + A_p P_{p,t} \right) \right\}.$$

Referring to (14), with fixed B_p, the network energy efficiency function is non-linear with ρ_1 and ρ_2. Thus, in the following section, the effections of ρ_1 and ρ_2 on the network energy efficiency is analyzed by numerical simulations.

IV. Numerical Simulation Results

In this section, we consider a two-tier HetNets consisted by MBSs and PBSs. The the effections of ρ_1 and ρ_2 on the network energy efficiency is simulated according to (14) as theoretical results. The Monte Carlo simulation is adopted to verify the theoretical results. The simulation parameters are summarized in Table I.

TABLE I: Simulation Parameters

Parameter	Value
Carrier frequency f	$2GHz$
Path loss exponent α	4
Path loss L	$L = 10\log(L_0) + \alpha 10\log(d_m)$ where $L_0 = (4\pi f/c)^2$, $c = 3\times10^8\ m/s$
MBS transmit power P_m or $P_{m,t}$	$43dBm$
PBS transmit power P_p or $P_{p,t}$	$30dBm$
Bandwidth W	$10MHz$
MBS static power $P_{m,s}$	$800W$
PBS static power $P_{p,s}$	$130W$
PBS CRE bias B_p	$3dBm$

The network energy efficiency versus ρ_1 with different ρ_2/ρ_1 and fixed UE density is shown in Fig. 2. The simulation results show that the curves of the theoretical simulation results can capture the Monte Carlo simulation results in practical scenario accurately, which verify the validity of our theoretical formulation. With different ρ_2/ρ_1, the curves of the network energy efficiency keep increasing with the increase of ρ_1 at the initial stage. Nonetheless, with ρ_1 further increasing, the curves of the network energy efficiency tend to decline due to the rise of power consumption caused by the increment of MBS density. Therefore, with fixed ρ_2/ρ_1 and UE density, there exits an optimal ρ_1 to maximize the network energy efficiency. Furthermore, the curve of the network energy efficiency with higher ρ_2/ρ_1 always outperforms that with lower ρ_2/ρ_1, which signifies that increase the ratio of PBS density to MBS density will be more energy efficient for HetNets.

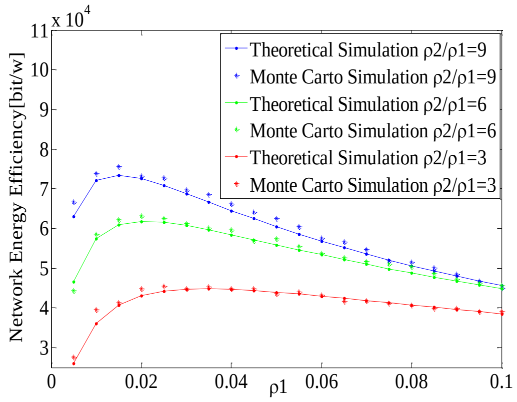

Fig. 2. The network energy efficiency versus ρ_1 with different ρ_2/ρ_1.

The network energy efficiency versus ρ_2 with different ρ_2/ρ_1 and fixed UE density is depicted in Fig. 3. It also shows that the network energy efficiency with higher ρ_2/ρ_1 performs better than that with lower ρ_2/ρ_1. And with the increase of ρ_2, the network energy efficiency curve will rise first and drop. This is due to the fact that too many PBSs deployed in the network will not only cause severe interference to users, but also cause a lot of power consumption, which make the network energy efficiency deteriorate severely. Therefore, the PBS density should be deployed carefully with the given UE density and ρ_2/ρ_1.

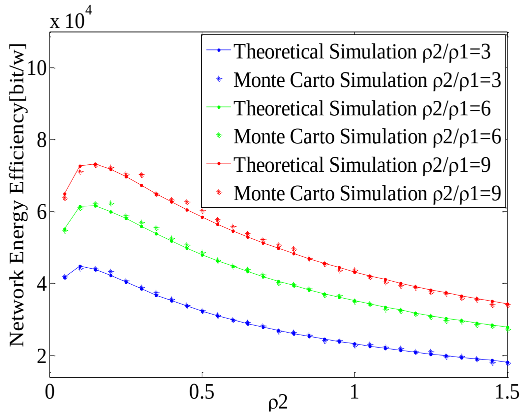

Fig. 3. The network energy efficiency versus ρ_2 with different ρ_2/ρ_1.

The relationship between the network energy efficiency and ρ_1 with different ρ_2 is depicted in Fig. 4. The theoretical results match the Monte Carlo simulation results very well. The network energy efficiency will keep decreasing with the increase of ρ_1. Hence, when the UE density and PBS density is given, the less MBSs are deployed in the HetNet, the higher network energy efficiency will be obtained.

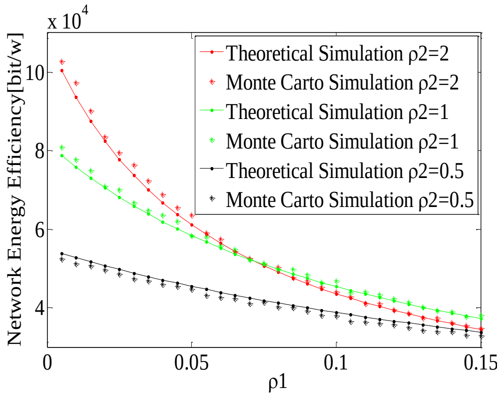

Fig. 4. The network energy efficiency versus ρ_1 with different ρ_2.

The impact of ρ_2 on the network energy efficiency with different ρ_1 is shown in Fig. 5. The network energy efficiency curve performs better with lower ρ_1 than that with higher ρ_1. And all the curves present convex with the increase of ρ_2. Therefore, there exists an optimal ρ_2 to maximize the network energy efficiency with fixed ρ_1 and UE density.

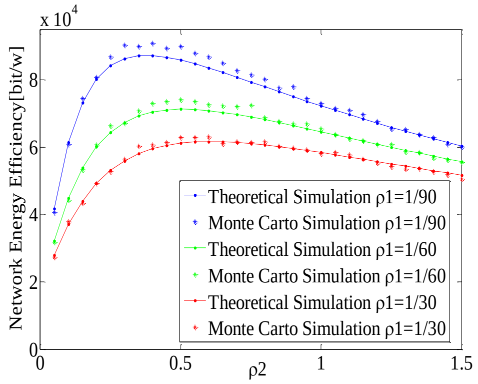

Fig. 5. The network energy efficiency versus ρ_2 with different ρ_1.

V. Conclusion

In this paper, we analyze the effections of the MBSs and PBSs densities on the network energy efficiency in a two-tier HetNets with eICIC. We first obtain the closed-form of network energy efficiency as a function of MBSs and PBSs densities by adopting stochastic geometry theory. Then, the theoretical derivation is verified by Monte Carto simulation. Simulation analysis show that the network energy efficiency can be improved by adjusting the reasonable densities of MBSs and PBSs. This work can provide a theoretical basis for the deployment of base stations in HetNets with eICIC.

References

[1] A. Damnjanovic, J. Montojo, Y. Wei, *et al.*, "A survey on 3GPP heterogeneous networks," *IEEE Wireless Commun.*, vol. 18, no. 3, pp. 10-21, 2011.

[2] T. Zhang, J. Zhao, L. An, and D. Liu, "Energy efficiency of base station deployment in ultra-dense HetNets: A stochastic geometry analysis," *IEEE Wireless Commun. Letters*, vol. 5, no. 2, pp. 184-187, 2016.

[3] K. Yamamoto and T. Ohtsuki, "Parameter optimization using local search for CRE and eICIC in heterogeneous network," in *Proc. 25th IEEE Annual International Symposium on Personal, Indoor, and Mobile Radio Commun.*, 2014, pp. 1536-1540.

[4] S. Singh, H. S. Dhillon, and J. G. Andrews, "Offloading in heterogeneous networks: Modeling, analysis, and design insights," *IEEE Trans. on Wireless Commun.*, vol. 12, no. 5, pp. 2484-2497, 2015.

[5] X. Chen, H. Xia, Z. Zeng, *et al.*, "Energy-efficient heterogeneous networks for green communications by inter-layer interference coordination," in *Proc. International Symposium on Wireless Personal Multimedia Commun.*, 2014, pp. 70-74.

[6] S. Deb, P. Monogioudis, J. Miernik, *et al.*, "Algorithms for enhanced inter-cell interference coordination (eICIC) in LTE HetNets," *IEEE/ACM Trans. on Networking*, vol. 22, no. 1, pp. 137-150, 2014.

[7] N. Bhushan, J. Li, D. Malladi, *et al.*, "Network densification: the dominant theme for wireless evolution into 5G," *IEEE Commun. Magazine*, vol. 52, no. 2, pp. 82-89, 2014.

[8] J. Feng, Z. Feng, Z. Wei, *et al.*, "Optimal base station density in ultra-densification heterogeneous network," in *Proc. IEEE Wireless Commun. and Networking Conf.*, 2015, pp. 1452-1457.

[9] S. Sarabjot and J. G. Andrews, "Joint resource partitioning and offloading in heterogeneous cellular networks," *IEEE Trans. on Wireless Commun.*, vol. 13, no. 2, pp. 888-901, 2014.

[10] N. Bhushan, J. Li, D. Malladi, *et al.*, "Network densification: the dominant theme for wireless evolution into 5G," *IEEE Commun. Magazine*, vol. 52, no. 2, pp. 82-89, 2014.

[11] L. Li, M. Peng, C. Yang, *et al.*, "Optimization of base-station density for high energy-efficient cellular networks with sleeping strategies," *IEEE Trans. on Vehicular Technology*, vol. 65, no. 9, pp. 7501-7514, 2016.

[12] H. Wu, N. Zhang, X. Tao, *et al.*, "Capacity- and Trust-aware BS Cooperation in Non-uniform HetNets: Spectral efficiency and optimal BS density," *IEEE Trans. on Vehicular Technology*, no. 99, p. 1, 2017.

[13] A. Lu, T. Zhang, and C. Feng, "Stochastic geometry based energy-efficient base station density optimization in cellular networks," in *Proc. IEEE Wireless Commun. and Networking Conf.*, pp. 1614-1619, 2015.

[14] X. Lin and S. Wang, "Joint user association and base station switching on/off for green heterogeneous cellular networks," in *Proc. IEEE International Conf. on Commun.*, pp. 1-6, 2017.

[15] X. Ge, S. Tu, G. Mao, *et al.*, "5G ultra-dense cellular networks," *IEEE Wireless Commun.*, vol. 23, no. 1, pp. 72-79, 2016.

[16] X. Lin and S. Wang, "Joint user association and base station switching on/off for green heterogeneous cellular networks," in *Proc. IEEE International Conf. on Commun.*, 2017, pp. 1-6.
[17] J. G. Andrews, F. Baccelli and R. K. Ganti, "A tractable approach to coverage and rate in cellular networks," *IEEE Trans. on Commun.*, vol. 59, no. 11, pp. 3122-3134, 2011.

Yanzan Sun received Ph.D. degree in Control Theory and Control Engineering from Tongji University, China, in 2011. From 2007 to 2009, he was an assistant researcher in Shanghai Research Center for Wireless Communication (Wico) and worked on spectrum sensing and dynamic spectrum allocation in cognitive radio networks. In 2009, he was awarded a National government study abroad scholarship to pursue his research as a visiting student in Electrical Engineering Department in Columbia University. From 2011 to 2012, he was a research Engineer in Huawei Technologies Co., Ltd. where he researched on enhanced Inter-cell Interference Coordination (eICIC) in 3GPP Long Term Evolution (LTE) systems. He is currently an assistant professor in School of Communications and information engineering in Shanghai University. His research interests include wireless communications, spectrum sensing, wireless spectrum resource allocation/management in cognitive networks and ICIC/eICIC in HetNets.

Wenqing Xia received B.E. degree (2015) in electronic engineering from JiLin University. Now she is a M.S. candidate in School of Communication and Information Engineering of Shanghai University. Her current research interests include green communication, resource management and eICIC in HetNets.

Yating Wu received her B.E. (2004), and Ph.D. (2009) degrees from Beijing University of Posts and Telecommunications, and Peking University, respectively. From 2009 to 2010, she worked as a senior research assistant in the Department of Electronic Engineering at City University of Hong Kong. She joined Shanghai University in 2011 and is currently a Lecturer in the Department of Communication Engineering. She is a member of China Broadband Wireless IP Standard Group (ChinaBWIPS) since 2011. Her current research interests include signal processing for wireless communications, cooperative MIMO communications and limited feedback techniques.

Tao Wang received Ph.D from Universite Catholique de Louvain (UCL), Belgium in 2012, Doctor of Engineering and Bachelor (summa cum laude) degrees from Zhejiang University, China, in 2006 and 2001, respectively. He has been with Department of Communication Engineering, Shanghai University as a Professor since Feb. 2013. His current interest is in resource allocation and adaptive modulation techniques for wireless communication and signal processing systems. He received Shanghai Eastern-Scholar Professorship Award from Shanghai Municipal Education Commission, as well as Best Paper Award in 2013 International Conference on Wireless Communications and Signal Processing. He is an associate editor for EURASIP Journal on Wireless Communications and Networking, Signal Processing: An International Journal (SPIJ), as well as an editorial board member of Recent Patents on Telecommunications. He served as a session chair in 2012 IEEE International Conference on Communications, 2013 IEEE \& CIC International Conference on Communications in China, and 2013 International Conference on Wireless Communications and Signal Processing. He was also a TPC member of International Congress on Image and Signal Processing in 2012 and 2010.

Yong Fang received the Ph.D. degree in Electronic Engineering from City University of Hong Kong, Hong Kong, in 1999. He is now a professor in School of Communication and Information Engineering, Shanghai University, Shanghai. His research interests include communication signal processing, blind signal processing and adaptive information system.